Analytic study of orthogonally polarized solitons interacting in highly birefringent optical fibers

J. Nathan Kutz

Program in Applied Mathematics, Princeton University, Princeton, New Jersey 08544, and Lucent Technologies and AT&T Research, Murray Hill, New Jersey 07974

Steffen D. Koehler, L. Leng, and Keren Bergman

Department of Electrical Engineering and Advanced Technology Center for Photonics and Opto-Electronic Materials, Engineering Quadrangle, Princeton University, Princeton, New Jersey 08544

Received March 22, 1996; revised manuscript received June 17, 1996

We examine analytically, numerically, and experimentally the phase shift incurred by a soliton pulse when it collides with a copropagating, orthogonally polarized soliton pulse in a highly birefringent optical fiber. Use of a well-known average variational principle and a Gaussian ansatz reduces the dynamics to a set of ordinary differential equations for which an approximate analytic solution is found in the case of highly birefringent fibers. The analytic approximation is shown to be in good agreement with the full numerical model and experimental data, allowing it to be used as an evaluation tool for the design of nonlinear optical loop mirror switches. © 1997 Optical Society of America [S0740-3224(97)02802-6]

1. INTRODUCTION

As the demand for higher bit rates in optical communications continues to grow, ultrafast switching and data processing methods for local area networks have become areas of increasingly focused research. Optical fibers are inexpensive, low-loss waveguides and exhibit the types of nonlinearity that can be exploited in making ultrafast all-optical switching devices. Fiber ring reflectors, also known as Sagnac interferometers, have proved to be most convenient and versatile for all-fiber switching implementations, and many devices have been demonstrated as demultiplexers of ultrafast optical pulses with high switching contrasts.[1–6]

One of the major drawbacks of all-fiber optic switches has been the long fiber lengths that are required by the extremely low nonlinear coefficient of silica. These long spans of fibers (≈1–5 km) have been a source of severe latency, which is unacceptable for systems implementation. As an alternative, we examine here soliton–soliton collisions in highly birefringent, polarization-maintaining fibers as a means of generating large nonlinear phase shifts in relatively short segments of fiber (2–10 m). Moores *et al.*[7,8] studied numerically and experimentally the interaction between two first-order orthogonally polarized solitary pulses in a polarization-maintaining fiber loop switch. Here we extend these studies to collisions between a higher-order ($N = 5$) soliton control pulse and a first-order orthogonally polarized signal pulse. Further, we present direct experimental measurements of the nonlinear phase shift imposed on the signal pulse during one collision.

Although the mechanism (cross-phase modulation) responsible for the collisional phase shift is well understood, numerical models are typically necessary to understand the complicated nonlinear dynamics of the soliton–soliton collision. We present a well-known average variational method that can be used to generate a reduced model for the pulse dynamics. The reduction allows the pulse dynamics to be described by a simple set of ordinary differential equations (ODE's). In an appropriate limit, these ODE's can be approximated by exact analytic solutions that are shown to be in good agreement with the experimental measurements and with the numerical results.

Formulation of the model, which includes the appropriate governing equations and scalings for the copropagating and orthogonally polarized solitons, is introduced in Section 2. Section 3 outlines the basic principles of the variational method as applied to the governing equations. The reduced set of equations is analyzed in Section 4, and an appropriate limit is explored that gives analytic results for the collisional phase shift. Section 5 compares numerical simulations with the reduced model and the analytic solution. Experimental results are discussed in Section 6. The paper concludes in Section 7 with a brief summary of the results.

2. FORMULATION

The evolution of orthogonally polarized optical pulses copropagating in a birefringent fiber is governed by the coupled nonlinear Schrödinger (NLS) equations[9–11]

$$i\frac{\partial u}{\partial z} + \frac{1}{2}\frac{\partial^2 u}{\partial t^2} + (|u|^2 + B|v|^2)u = 0 \qquad (1a)$$

0740-3224/97/030636-07$10.00

$$i\left(\frac{\partial v}{\partial z} - \delta\frac{\partial v}{\partial t}\right) + \frac{1}{2}\frac{\partial^2 v}{\partial t^2} + (|v|^2 + B|u|^2)v = 0, \quad (1b)$$

where u represents the signal pulse and v the orthogonally polarized control pulse, and Eqs. (1) are written in the rest frame of the signal pulse. The variable t represents the time in the rest frame of the signal divided by the pulse width $t_0 = 200$ fs (full width at half-maximum), u and v are the field envelopes divided by the peak field amplitude of the signal pulse E_0, and z is the physical distance divided by the dispersion length z_0 such that

$$|E_0|^2 = \frac{\lambda_0 A_{\text{eff}}}{2\pi n_2 \omega_0 z_0} \quad (2)$$

gives the peak power of a one-soliton pulse and

$$z_0 = \left(\frac{t_0}{1.76}\right)^2 \frac{2\pi c}{\lambda_0{}^2|D|} = 0.84 \text{ m}. \quad (3)$$

Here $D \approx 12$ ps/(km nm) is the group-velocity-dispersion coefficient, n_2 is the nonlinear coefficient of the fiber, A_{eff} is the effective cross-sectional area of the fiber, and $\lambda_0 = 1.55$ μm and c are the carrier's wavelength and the free-space speed of light, respectively. The parameter δ in Eqs. (1) is a scaled measure of the group-velocity difference (slip) between the fast and the slow axes and is given by

$$\delta = z_0\frac{1.76}{t_0}\left(\frac{1}{V_g{}^u} - \frac{1}{V_g{}^v}\right) \approx \frac{\Delta n z_0}{c}\frac{1.76}{t_0} = 12.38, \quad (4)$$

where $V_g{}^u$ and $V_g{}^v$ are the group velocities of the signal and the control pulses, respectively ($\mathrm{d}k/\mathrm{d}\omega = 1/V_g$), and it is assumed in the last approximate equality that $\Delta n \approx 5 \times 10^{-4} \gg \omega(\mathrm{d}/\mathrm{d}\omega)(\Delta n)$. This final assumption requires that $(\mathrm{d}/\mathrm{d}\omega)(\Delta n) \ll 10^{-18}$. Although this assumption is not completely justified, we adopt it here and discuss it further in Section 6.

In linearly birefringent fiber, which is of interest here, $B = 2/3$, and Eqs. (1) are no longer integrable by the inverse-scattering transform.[12] This is in contrast to the uncoupled NLS equation ($B = 0$), which is valid for both the u and the v dynamics when the pulses are well separated. As a result, the coupled NLS equations no longer support solitons in the strict mathematical sense; rather, solitonlike pulses are observed.[13] However, in the remainder of this paper we refer to these solitonlike pulses as solitons.

For well-separated and noninteracting soliton pulses the dynamics of both the u and v pulses reduce to the standard NLS equation for which the soliton solutions are well known. In particular, the one-soliton solution for the signal pulse is simply given by

$$u = \text{sech}(t)\exp(iz/2). \quad (5)$$

There is no loss in generality in assuming a solution of this form because the NLS equation can always be transformed to bring any single soliton to this form. Thus a one-soliton pulse will experience a phase shift (linear in z) that is due to the $\exp(iz/2)$ phase factor, which is a result of self-phase modulation (SPM). The situation is much more complicated for interacting pulses.

In general, the dynamics of the nonlinear interaction between colliding pulses as given by Eqs. (1) is difficult to understand analytically inasmuch as it involves a complex set of interactions among various physical effects. Thus one is often left with numerical simulations of Eqs. (1) as the only tool with which to explore the dynamics. Such numerical simulations are computationally expensive and do not provide insight into how the various physical effects contribute to the dynamics. We therefore introduce an average variational method that reduces the two nonlinear partial differential equations to an appropriate set of ODE's. We show that the reduced model lends significant insight and computational savings to the full equations [Eqs. (1)] and further provides an analytical solution for the collisional phase shift in the case of high-birefringence fiber.

3. VARIATIONAL METHOD

The average variational method[14] used here was introduced by Anderson[15] for a better understanding of the NLS equation. It was later used by Ueda and Kath,[13] Wang *et al.*,[11] and Kaup *et al.*[16] for coupled NLS equations (1). The essential idea of the variational method involves choosing an appropriate pulse-shape ansatz whose free parameters are allowed to vary as a function of distance. Provided that the ansatz and the associated free parameters are chosen in a reasonable fashion, the variational method can provide quite accurate results[11,13,15,16] and lend significant insight into the nonlinear pulse dynamics.

Although the variational method is outlined elsewhere,[13,15] we include a brief summary of it here for completeness. The fundamental physical principle involved in this approach is rooted in Lagrangian methods for classical mechanics,[17,18] i.e., particle trajectories follow a path of least resistance. This requires the dynamics to minimize a certain energy integral (Hamilton's principle), which leads to the well-known Euler–Lagrange equations[17,18] of classical mechanics. We restate the governing coupled NLS equations (1) in terms of their Lagrangian form. Here the appropriate Lagrangian is[11,13]

$$L = \int_{-\infty}^{\infty} \mathcal{L}(u, u^*, v, v^*)\mathrm{d}t, \quad (6)$$

where $\mathcal{L}$ is the Lagrangian density, given by

$$\begin{aligned}\mathcal{L} = {} & i\left(u\frac{\partial u^*}{\partial z} - u^*\frac{\partial u}{\partial z}\right) + i\left(v\frac{\partial v^*}{\partial z} - v^*\frac{\partial v}{\partial z}\right) \\ & - i\delta\left(v\frac{\partial v^*}{\partial t} - v^*\frac{\partial v}{\partial t}\right) - \frac{4}{3}|u|^2|v|^2 \\ & + \left(\left|\frac{\partial u}{\partial t}\right|^2 - |u|^4\right) + \left(\left|\frac{\partial v}{\partial t}\right|^2 - |v|^4\right). \end{aligned} \quad (7)$$

We determine the Lagrangian density by requiring the parameters u and v to obey the variational principle such that

$$\frac{\delta\mathcal{L}}{\delta p} = \frac{\partial}{\partial z}\left(\frac{\partial\mathcal{L}}{\partial p_z}\right) + \frac{\partial}{\partial t}\left(\frac{\partial\mathcal{L}}{\partial p_t}\right) - \frac{\partial\mathcal{L}}{\partial p} = 0, \quad (8)$$

where $p = u, u^*, v, v^*$, with $\partial/\partial p_z = \partial/\partial(\mathrm{d}p/\mathrm{d}z)$ and $\partial/\partial p_t = \partial/\partial(\mathrm{d}p/\mathrm{d}t)$.

Given then an initial ansatz with appropriately chosen free parameters (i.e., amplitude, width, central position, etc.), the Lagrangian L can be evaluated by means of Eq. (6). We can find a reduced system of ODE's by recalling that the free parameters are functions of z. Therefore variations with respect to each of the free parameters satisfy the Euler–Lagrange equations,[17,18] so

$$\frac{\delta L}{\delta \rho} = \frac{\mathrm{d}}{\mathrm{d}z}\left(\frac{\partial L}{\partial \rho_z}\right) - \frac{\partial L}{\partial \rho} = 0, \tag{9}$$

where ρ is an ansatz free parameter and $\partial/\partial\rho_z = \partial/\partial(\mathrm{d}p/\mathrm{d}z)$. This reduces the complicated coupled NLS equations to a simplified system of ODE's.

The particular case of a hyperbolic secant ansatz has been studied extensively by Ueda and Kath[13] and by Wang *et al.*[11] In both cases the dynamics were reduced to a set of eight coupled ODE's that give relatively accurate results at a fraction of the computational expense of Eqs. (1). However, one is still left with a computational problem for the reduced system because an analytical solution of the reduced ODE's is intractable.

In the reduced model developed here we assume that the fundamental interaction occurs between the phase and the central position parameters. We can obtain further simplification by assuming that the pulses have a Gaussian rather than a hyperbolic secant shape.[15,16] This gives an ansatz of the form

$$u = \eta \exp\left[-\left(\frac{t - t_1}{W}\right)^2\right]\exp\{i[V_1(t - t_1) + \phi_1]\}, \tag{10a}$$

$$v = A\eta \exp\left[-\left(\frac{t - t_2}{W}\right)^2\right]\exp\{i[V_2(t - t_2) + \phi_2]\}, \tag{10b}$$

where A ($\geqslant 1$), η, and W are real, fixed constants and the six free parameters that depend on z are V_i, t_i, and ϕ_i ($i = 1, 2$). These three parameters represent the velocity of the central position, the central position, and the cumulative phase, respectively, of the Gaussian pulse.

In general, approximating the nearly hyperbolic secant profiles by Gaussian profiles leads to errors in the reduced dynamics. However, this error can be substantially reduced by appropriate choices of the parameters η and W. In particular, we require the pulse energy ($\int |u|^2 \mathrm{d}t$) to be equivalent in the cases of both a hyperbolic secant and a Gaussian ansatz. Making use of Eq. (10a) and it hyperbolic secant counterpart, we find that

$$\int |u_{\text{hyperbolic secant}}|^2 \mathrm{d}t = 2, \tag{11a}$$

$$\int |u_{\text{Gaussian}}|^2 \mathrm{d}t = (\pi W/2)^{1/2}\eta^2. \tag{11b}$$

Requiring the pulse energy to be equal in either case leads to the condition

$$\sqrt{2\pi W}\,\eta^2 = 4. \tag{12}$$

Note here that the parameter A in Eq. (10b) corresponds to the usual soliton amplitude given for the hyperbolic secant ansatz, i.e., an $N = 3$ soliton corresponds to $A = 3$. The criterion in Eq. (12) is important, as the phase shift that is due to collision is strongly dependent on the total energy of the control pulse as opposed to the actual pulse shape. A second equation involving η and W will be derived below, allowing for the explicit evaluation of each.

The Lagrangian L as given by Eq. (6) can now be evaluated by use of the ansatz of Eqs. (10) and the variations as given by Eq. (9). The complicated set of partial differential equations [Eqs. (1)] reduces to a simple set of four coupled ODE's:

$$\frac{\mathrm{d}t_1}{\mathrm{d}z} = V_1, \tag{13a}$$

$$\frac{\mathrm{d}t_2}{\mathrm{d}z} = V_2 - \delta, \tag{13b}$$

$$\frac{\mathrm{d}V_1}{\mathrm{d}z} = \frac{2\sqrt{2}A^2\eta^2}{3\sqrt{W}}(t_2 - t_1)\exp\left[-\frac{(t_1 - t_2)^2}{W}\right], \tag{13c}$$

$$\frac{\mathrm{d}V_2}{\mathrm{d}z} = \frac{2\sqrt{2}\eta^2}{3\sqrt{W}}(t_1 - t_2)\exp\left[-\frac{(t_1 - t_2)^2}{W}\right]. \tag{13d}$$

Note that the parameters ϕ_1 and ϕ_2 do not appear in Eqs. (13) because they are completely determined by the remaining parameters of the problem, i.e., A, η, W, V_i, and t_i.

Before proceeding to discuss the phase shift incurred from a collision, we first calculate the total phase shift acquired by the signal pulse. The phase shift incurred by the pulse is captured by the parameter ϕ_1, which we determine by requiring that the ansatz in Eqs. (10) satisfy coupled NLS equations (1). Plugging Eqs. (10) into Eqs. (1) then gives

$$\begin{aligned}\phi_1 = -\frac{z}{W} + \int_0^z \mathrm{d}z\Bigg\{ & \frac{1}{2}V_1^2 + \frac{2}{W^2}(t - t_1)^2 \\ & + \eta^2 \exp\left[\frac{-2}{W}(t - t_1)^2\right] + \frac{2}{3}A^2\eta^2 \\ & \times \exp\left[\frac{-2}{W}(t - t_2)^2\right] - \frac{2\sqrt{2}A^2\eta^2}{3\sqrt{W}} \\ & \times (t - t_1)(t_2 - t_1)\exp\left[-\frac{(t_1 - t_2)^2}{W}\right]\Bigg\},\end{aligned} \tag{14}$$

where it is assumed that $\phi_1 = 0$ at $z = 0$. A similar expression can be obtained for the parameter ϕ_2, which is the cumulative phase of the control pulse.

4. COLLISIONAL PHASE SHIFT

The averaged variational principle produces a reduced set of equations that provides a greatly simplified description of the pulse dynamics. In particular, on assuming the Gaussian ansatz in Eqs. (10), we arrived at the four coupled ODE's given by Eqs. (13) with the cumulative

phase shift given by Eq. (14). We can further simplify the reduced model by noting that

$$t_2 = -\frac{t_1}{A^2} - \delta z + \Delta t, \tag{15a}$$

$$V_2 = -\frac{V_1}{A^2}, \tag{15b}$$

where it is assumed that $t_1 = 0$ at $z = 0$ and $t_2 = \Delta t$ at $z = 0$, so the initial signal pulse and control pulse separation is Δt. Thus the four coupled ODE's have been reduced to just two coupled ODE's involving t_1 and V_1:

$$\frac{dt_1}{dz} = V_1, \tag{16a}$$

$$\frac{dV_1}{dz} = -\frac{2\sqrt{2}A^2\eta^2}{3\sqrt{W}}[t_1(1 + 1/A^2) + \delta z - \Delta t] \times \exp\left\{-\frac{[t_1(1 + 1/A^2) + \delta z - \Delta t]^2}{W}\right\}. \tag{16b}$$

Once solutions for V_1 and t_1 are obtained, the control pulse parameters V_2 and t_2 can easily be determined from Eqs. (15).

In general, Eqs. (16) are difficult to solve analytically. However, numerical simulations of Eqs. (1) show that the central position of the signal pulse is shifted only slightly by the rapid collision between the control and signal pulses. From this observation it is reasonable to assume that t_1 remains small after the collision. This approximation greatly simplifies Eq. (16b) because then

$$t_1(1 + 1/A^2) \ll 2t_1 \ll 1, \tag{17}$$

and the approximate equation for the parameter V_1 reduces to

$$\frac{dV_1}{dz} \approx -\frac{2\sqrt{2}A^2\eta^2}{3\sqrt{W}}(\delta z - \Delta t)\exp\left[-\frac{(\delta z - \Delta t)^2}{W}\right]. \tag{18}$$

A simple integration then yields the solution of relation (18):

$$V_1 \approx \frac{\sqrt{2W}A^2\eta^2}{3\delta}\exp\left[-\frac{(\delta z - \Delta t)^2}{W}\right], \tag{19}$$

so, for $t_1 \ll 1$, both V_1 and t_1 can be evaluated explicitly.

We now address the approximation of inequality (17) concerning the size of t_1. To this end, we evaluate t_1, using relation (19). From Eq. (16a) we find that for some length of fiber L

$$t_1 \approx \frac{\sqrt{2W}A^2\eta^2}{3\delta}\int_0^L \exp\left[-\frac{(\delta z - \Delta t)^2}{W}\right]dz. \tag{20}$$

If initially the pulses are well separated (a few pulse widths apart) and if after a length L the pulses have collided and once again are well separated, the integral in relation (20) can be approximated by a complete integral. The integral is then evaluated explicitly, giving the signal's central position shift as

$$t_1 \approx \frac{\sqrt{2\pi}W\eta^2}{3}\left(\frac{A}{\delta}\right)^2 = \frac{4\sqrt{W}}{3}\left(\frac{A}{\delta}\right)^2, \tag{21}$$

where use has been made of Eq. (12). We can then determine the parameter regime for which the approximations given by relations (19) and (20) are valid. In particular, the fundamental assumption was that $t_1 \ll 1$, which from relation (21) implies that

$$A/\delta \ll 1. \tag{22}$$

Thus the approximation holds as long as the interaction is rapid, i.e., the slip parameter δ is large and the initial control pulse amplitude is not too high.

The evaluation of the corresponding phase shift given by Eq. (14) is difficult and requires numerical integration. However, in keeping with the spirit of the above approximation, the phase-shift calculation can also be greatly simplified in the $t_1 \ll 1$ limit. Thus, for $t_1 \ll 1$, the phase shift at the center of the signal pulse ($t = 0$) is

$$\phi_1 \approx z\left(\eta^2 - \frac{1}{W}\right) + \frac{2A^2\eta^2}{3}\int_0^z \exp\left[\frac{-2}{W}(\delta z - \Delta t)^2\right]dz. \tag{23}$$

Notice that the cumulative phase shift is essentially given by a linear (in z) contribution and an integrated contribution that is due to collision. Specifically, the first term on the right-hand side of relation (23) gives the self-phase shift expected from the NLS equation (5) that is due to SPM. Until now, the parameters W and η have been arbitrary. However, we can fix these constants by noting that the phase shift of the signal pulse for well-separated pulses should match the SPM contribution of the single-soliton pulse as given by Eq. (5). This requires that

$$\left(\eta^2 - \frac{1}{W}\right) = \frac{1}{2}, \tag{24}$$

which gives a second equation involving W and η. Making use of Eq. (12), we find that

$$\eta_{\pm} = \left[\frac{2}{\pi}(2 \pm \sqrt{4 - \pi})\right]^{1/2}. \tag{25}$$

By considering the η_+ case, we find that $\eta = 1.3649$ and $W = 0.7336$ (the η_- case gives $\eta = 0.8267$ and $W = 5.4519$ and can be used equally well).

We can evaluate the integral in relation (23) by assuming that the lower limit of integration can be approximated by $-\infty$. Inasmuch as the Gaussian is localized about $z = \Delta t/\delta$, this is a good approximation. Further, if we recall that $A/\delta \ll 1$, we find that the cumulative phase shift is given by

$$\phi_1 \approx \frac{z}{2} + \frac{4A^2}{6\delta}\{\mathrm{erf}[\sqrt{2/W}(\delta z - \Delta t)] + 1\}, \tag{26}$$

where erf( ) is the standard error function.[19] In practice, we are interested only in the total collisional phase shift incurred by the signal pulse. In this case erf( ) $\to 1$, and the collisional phase shift (which is due to cross-phase modulation only) is given by

$$\phi_{\mathrm{collision}} = \frac{4A^2}{3\delta} = \frac{2\lambda^2|D|A^2}{3\pi\Delta n(t_0/1.76)}, \tag{27}$$

where we have subtracted the phase shift ($z/2$) that is due to SPM, i.e., the first term on the right-hand side of relation (26). Note that the final analytic expression is given in terms of the relevant physical parameters, i.e., wavelength, dispersion, pulse width, and initial control pulse amplitude.

Thus, through the averaged Lagrangian formulation, we have been able to reduce the dynamics of the soliton collision to a simple system of ODE's that in the appropriate limit ($A/\delta \ll 1$) reduces the collisional phase shift to the simple algebraic expression given by Eq. (27). Although several approximations are involved in deriving Eq. (27), they will be shown in Section 5 to be quite accurate in determining the collisional phase shift experienced by the signal pulse. Finally, it should be noted that soliton perturbation theory can also be used in evaluating the collisional phase shift. However, the result is given in terms of a nontrivial integral, which must be evaluated numerically, and its range of validity is not clear.

5. NUMERICAL RESULTS

To verify the analytic approximations made in Sections 5 and 6, we carry out extensive numerical simulations. Specifically, the accuracy of the reduced set of ODE's given by Eqs. (13) is explored. Further, the approximations that give rise to relations (26) and Eq. (27) in the limit of $A/\delta \ll 1$ are investigated. Unless stated otherwise, the parameter values used in the simulations are $D = 12$ ps/(km nm), $\Delta n = 5 \times 10^{-4}$, $t_0 = 200$ fs, and $\lambda_0 = 1.55$ μm. Initially, the pulses are separated by ≈ 1.7 ps. The numerical routine used to simulate Eqs. (1) utilizes a fourth-order Runge–Kutta method in time and a filtered pseudospectral method in space.[20] This procedure combines the advantages of split-step[21] and explicit Runge–Kutta[22] methods, yielding a relatively simple fourth-order scheme with improved numerical stability. The reduced system given by Eqs. (13) is numerically solved by the same fourth-order Runge–Kutta method as that used in the partial differential equation solver for Eqs. (1).

In Fig. 1 the initial pulse profile and the final (time-shifted) pulse profile are depicted, along with the phase shift incurred in a collision with an $A = 3$ soliton control pulse (left-axis label). Note once again that the one-soliton signal pulse is relatively unaffected by the collision. Specifically, the pulse simply is shifted by ≈ 8 fs. It should be noted that relation (21) predicts a time shift of ≈ 7.5 fs. The collisional phase shifts calculated from the full numerical simulations, the reduced ODE model, and the analytic expression in Eq. (27) are also plotted (right-axis label) and are seen to be in good agreement with one another.

Before proceeding to ascertain the errors incurred in the analytic model as given by relation (26), we make a comparison between the reduced model and the approximations that give rise to relation (26) and Eq. (27). In particular, Fig. 2 compares the system of ODE's as given by Eqs. (16) and its approximate solutions ($A/\delta \ll 1$) as given by relations (19) and (20) for various values of the control pulse amplitude A ($=1, 3, 5$). The top two figures in Fig. 2 depict the instantaneous central velocity shift (V_1) and the central position shift (t_1) for the case $A = 1$. The analytic approximation (dotted curves) is observed to be in good agreement with the ODE model (solid curves). It is clear from the middle two figures ($A = 3$) and the bottom two figures ($A = 5$) that the approximation begins to break down as the value of A increases.

We now provide a direct comparison of the collisional phase shifts as predicted from numerical simulations of Eqs. (1), from the ODE model of Eq. (14), and from the analytic approximation of Eq. (27). We subtract the SPM-contribution to the phase shift and consider only the

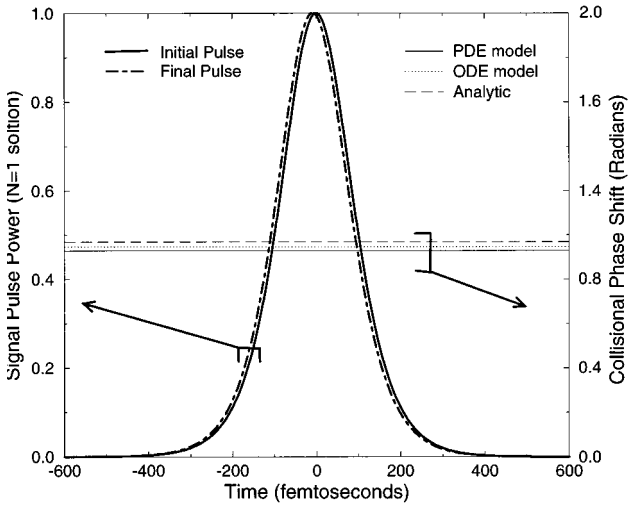

Fig. 1. Comparison of the initial and the final pulse amplitudes that are due to a collision with a three-soliton pulse (left-axis label) along with a comparison of the collisional phase shifts calculated from the three models (right-axis label). Note that the final pulse is time shifted by ≈ 8 fs.

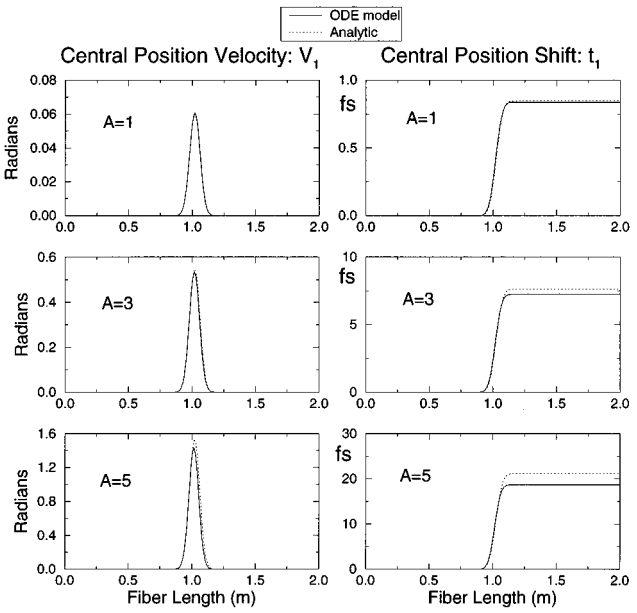

Fig. 2. Comparison of the ODE solutions for the pulse parameters that represent the signal's central position velocity (V_1) and central position (t_1) and its approximate solutions (dotted curves). Note that as A/δ increases, the agreement degrades.

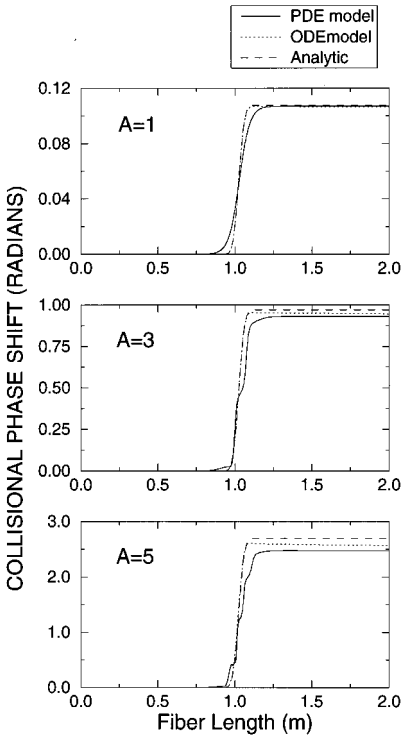

Fig. 3. Nonlinear phase shift computed by means of the full coupled NLS equations (PDE model, solid curves), the reduced ODE model (dotted curves), and the approximation to the ODE model (dashed curves) for $A = 1, 3, 5$. Much of the error observed in the case $A = 1$ arises from the Gaussian (as opposed to a hyperbolic secant) ansatz approximation.

collisional phase shift incurred in the soliton–soliton interaction. Various values of the control pulse amplitude A are considered. In Fig. 3 we plot the collisional phase shift calculated from the the full coupled NLS equations (1) (solid curves), the collisional phase shift from Eq. (14), which is calculated from the ODE model (dotted curves), and finally the analytic approximation to the collisional phase shift as given by relation (26) (dashed curves) for three values of A (=1, 3, 5). Note that the agreement between the reduced model and the analytic approximation corresponds well to the full numerical solution. Even in the case when $A = 5$ and the parameter $A/\delta = 0.404$ (so it is not much less than unity), the agreement is relatively good. This is remarkable considering that we reduced an infinite-dimensional partial differential equation system to a simple two-degrees-of-freedom model whose approximate phase shift can be calculated explicitly.

Thus the simple reduced model is shown to capture the essence of the nonlinear interaction, i.e., the shifts in central position and phase. This leading-order behavior further captures, through relations (19) and (21) and Eq. (27), the fundamental dependence of the interactions on the physical parameters of interest, such as the control pulse amplitude A, the dispersion value D, the pulse width t_0, and the birefringence strength Δn.

6. EXPERIMENTAL RESULTS

We measure the collisional phase shift experimentally by launching three optical pulses with $t = 1$ (i.e., FWHM $= 200$ fs) and $\lambda = 1.55$ μm into a 2-m length of Fujikura PANDA (polarization-maintaining) fiber. In this fiber, $D \approx 15$ ps/(km nm) and $\Delta n \approx 5 \times 10^{-4}$. We used the idler beam of a Coherent Optical parametric amplifier pumped by a regeneratively amplified mode-locked Ti:sapphire laser, producing pulses at a repetition rate of 200 kHz. This beam was split into three pulses that were recombined before being launched into the fiber. The first pulse, polarized along the fast axis of the fiber, is a reference pulse. The second pulse is the control pulse, which is polarized along the slow axis of the fiber and has a variable amplitude. The control follows the reference pulse by approximately 1 ns. The third pulse, whose amplitude is set such that it forms an $N = 1$ soliton in the fiber, is the signal pulse. The signal pulse is polarized along the fast fiber axis and is delayed with respect to the control pulse such that the birefringence of the fiber causes the signal pulse to overtake the control pulse inside the fiber.

The control pulse is modulated at 400 Hz and is separated from the signal and the reference pulses after the fiber by a polarizing beam splitter. The signal and the reference pulses are then interfered to permit us to measure the phase change on the signal induced by the control pulse. This collisional phase shift is depicted in Fig. 4 as a function of control pulse intensity. The vertical lines in the figure indicate integral soliton orders in the control pulse intensity. We compare the experimental results with the analytical model of Eq. (27) and the full numerical simulations of Eqs. (1). As is expected from the description in Section 5, the full numerical simulations and the analytic expression are in good agreement. Recall that in relation (4) we assumed that $\Delta n \gg \omega(\mathrm{d}/\mathrm{d}\omega)(\Delta n)$, which appears to be a reasonable assumption based on the analytical and experimental agreement. Finally, note that the measured collisional phase shifts depend almost linearly on the control pulse intensity, as predicted by Eq. (27).

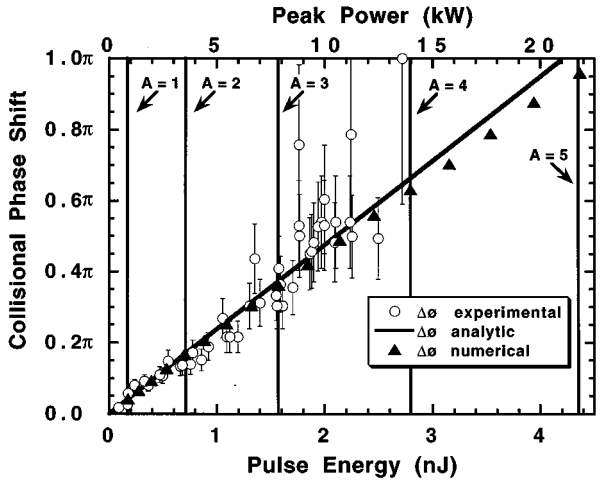

Fig. 4. Experimental, numerical, and analytic evaluation of the collisional phase shift of a first-order signal soliton caused by collision with a control pulse as a function of control pulse energy and peak power. The vertical lines depict the energies corresponding to integral soliton orders in the control pulse.

7. SUMMARY AND CONCLUSIONS

In conclusion, it has been shown that the dynamics that dictate the interaction of copropagating, orthogonally polarized soliton pulses can be significantly simplified by means of the variational formulation. The particular case of highly birefringent fiber allows for further simplification because the soliton–soliton collision is rapid and the leading-order effects of the collision are simply to shift the phase and the central position of the soliton pulses.

By use of a Gaussian ansatz, the variational formulation of the pulse evolution reduces to a simple set of coupled ODE's, which in the limit $A/\delta \ll 1$ (high birefringence) gives a simple analytic expression for the collisional phase shift. Note that the same analytic reduction is not expected with the use of a hyperbolic secant ansatz. Thus one can use the Gaussian ansatz to evaluate the phase shift experienced by the soliton signal pulse as the result of a collision with the soliton control pulse. Specifically, Eq. (27) gives the phase shift of the signal pulse that is due to a collision with an arbitrary amplitude control pulse.

Although the results given by the ODE model and by the analytic approximation are greatly simplified, they are shown to be in good agreement with both full numerical simulations and experimental results. Thus the simplified analytic expression in Eq. (27) proves to be a valuable tool for modeling and evaluating the leading-order behavior of nonlinear optical loop mirror switches, a design that relies on the soliton–soliton collisions.

This model has not included any higher-order effects that may further degrade the simplified model. In particular, the effect of intrapulse Raman scattering is expected to contribute to the pulse dynamics when pulse widths are of the order of hundreds of femtoseconds. These effects are being considered at present along with an analysis of the full nonlinear optical loop mirror switch.

ACKNOWLEDGMENTS

We gratefully acknowledge support from the National Science Foundation (ECS-9502491). J. N. Kutz acknowledges support from a National Science Foundation University–Industry Postdoctoral Fellowship (DMS-9508634).

REFERENCES

1. N. J. Doran and D. Wood, "Nonlinear-optical loop mirror," Opt. Lett. **13**, 56–58 (1988).
2. M. N. Islam, E. R. Sunderman, R. H. Stolen, W. Pleibel, and J. R. Simpson, "Soliton switching in a fiber nonlinear loop mirror," Opt. Lett. **14**, 811–813 (1989).
3. B. P. Nelson, K. J. Blow, P. D. Constantine, N. J. Doran, J. K. Lucek, I. W. Marshall, and K. Nelson, "All-optical Gbit/s switching using nonlinear optical loop mirror," Electron. Lett. **27**, 704–705 (1991).
4. N. A. Whitaker, Jr., M. C. Gabriel, H. Avramopoulos, and A. Huang, "All-optical, all-fiber circulating shift register with an inverter," Opt. Lett. **16**, 1999–2001 (1991).
5. M. Jinno and T. Matsumoto, "Ultrafast all-optical logic operations in a nonlinear Sagnac interferometer with two control beams," Opt. Lett. **16**, 220–222 (1991).
6. J. K. Lucek and K. Smith, "All-optical signal regenerator," Opt. Lett. **18**, 1226–1228 (1993).
7. J. D. Moores, K. Bergman, H. A. Haus, and E. P. Ippen, "Demonstration of optical switching by means of solitary wave collisions in a fiber ring reflector," Opt. Lett. **16**, 138–140 (1991).
8. J. D. Moores, K. Bergman, H. A. Haus, and E. P. Ippen, "Optical switching using fiber ring reflectors," J. Opt. Soc. Am. B **8**, 594–601 (1991).
9. C. R. Menyuk, "Pulse propagation in an elliptically birefringent Kerr media," IEEE J. Quantum Electron. **25**, 2674–2682 (1989).
10. C. R. Menyuk, "Nonlinear pulse propagation in birefringent optical fibers," IEEE J. Quantum Electron. **QE-23**, 174–176 (1987).
11. Q. Wang, P. K. A. Wai, C.-J. Chen, and C. R. Menyuk, "Numerical modeling of soliton-dragging logic gates," J. Opt. Soc. Am. B **10**, 2030–2039 (1993).
12. A. C. Newell, *Solitons in Mathematics and Physics* (Society for Industrial and Applied Mathematics, Philadelphia, Pa., 1985), Chap. 3, pp. 72–87.
13. T. Ueda and W. L. Kath, "Dynamics of coupled solitons in nonlinear optical fibers," Phys. Rev. A **42**, 563–571 (1990).
14. G. B. Whitham, *Linear and Nonlinear Waves* (Wiley-Interscience, New York, 1974), Chap. 14.
15. D. Anderson, "Variational approach to nonlinear pulse propagation in optical fibers," Phys. Rev. A **27**, 3135–3145 (1983).
16. D. J. Kaup, B. A. Malomed, and R. S. Tasgal, "Internal dynamics of a vector soliton in a nonlinear optical fiber," Phys. Rev. E **48**, 3049–3053 (1993).
17. H. Goldstein, *Classical Mechanics* (Addison-Wesley, Reading, Mass., 1980), Chap. 2.
18. L. D. Landau and E. M. Lifshitz, *Mechanics* (Pergamon, London, 1976), Chap. 1.
19. W. H. Beyer, ed., *CRC Standard Mathematical Tables* (CRC, Boca Raton, Fla., 1981), pp. 527–536.
20. T. Y. Hou, J. S. Lowengrub, and M. J. Shelley, "Removing the stiffness from interfacial flows with surface tension," J. Comput. Phys. **114**, 312–338 (1994).
21. M. D. Feit and J. A. Fleck, "Light propagation in graded-index optical fibers,"Appl. Opt. **17**, 3990–3998 (1978).
22. T. R. Taha and M. J. Ablowitz, "Analytical and numerical aspects of certain nonlinear evolution equations. II. Numerical, nonlinear Schrödinger equation," J. Comput. Phys. **55**, 203–230 (1984).